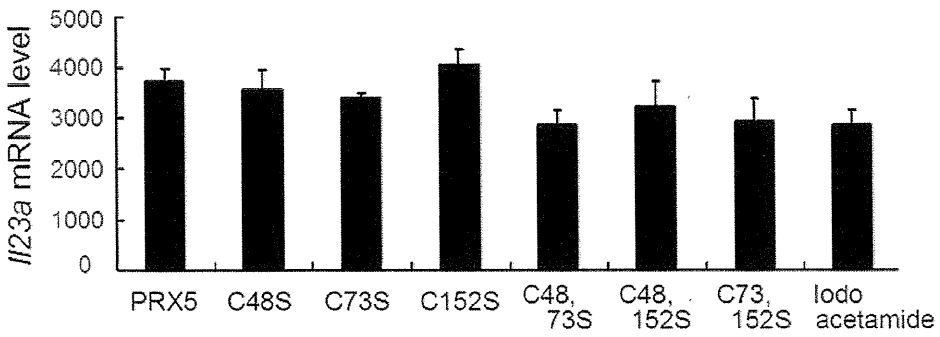

Supplementary Figure 7. The IL-23p19-inducing activity of point-mutated PRX5 protein and alkylated PRX5 protein by iodoacetamide in BMDC (*n* = 3, each).

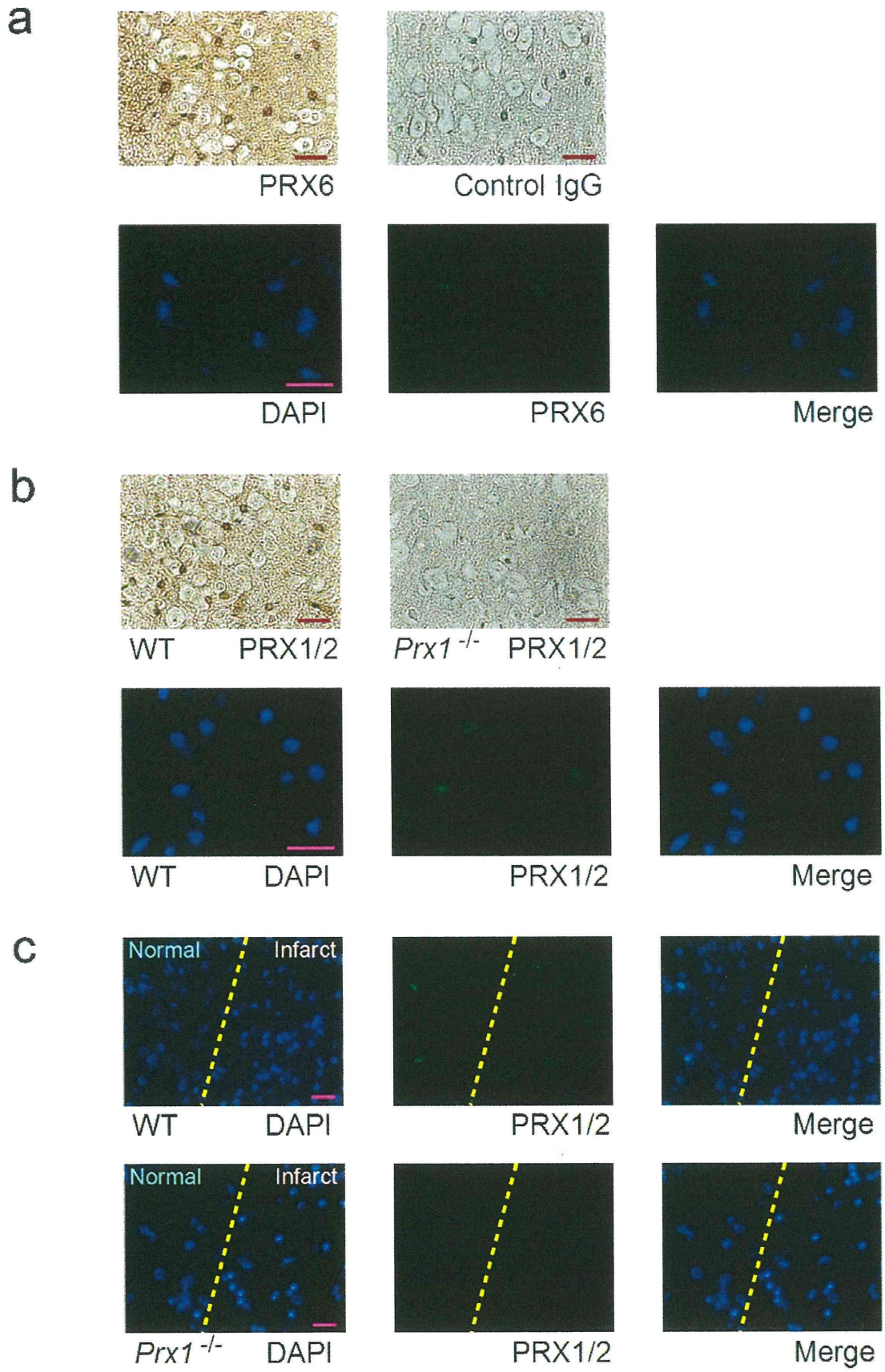
a
PRX6
Control IgG
DAPI
PRX6
Merge
b
WT
PRX1/2
Prx1 -/-
PRX1/2
WT
DAPI
PRX1/2
Merge
c
Normal
Infarct
WT
DAPI
PRX1/2
Merge
Normal
Infarct
Prx1 -/-
DAPI
PRX1/2
Merge

Supplementary Figure 8. (**a**) Anti-Prx6 immunohistostaining of normal brain tissue detected by DAB (upper panel) or Alexa Fluor 488 (lower panel). Control IgG was used for negative control. The pattern of anti-Prx6 immunostaining was similar to previous report[1]. We could find anti-Prx6 positive cells by high sensitivity imaging (lower panel), although this fluorescence intensity was weak compared to Prx6-positive debris (**Fig.2b**) (bar: 20 μm). (**b**) Anti-Prx1/2 immunohistostaining of normal brain tissue detected by DAB (upper panel) or Alexa Fluor 488 (lower panel). (bar: 20 μm) (**c**) Anti-Prx1/2 immunohistostaining of day 1 ischemic brain tissue detected by Alexa Fluor 488. (bar: 20 μm)

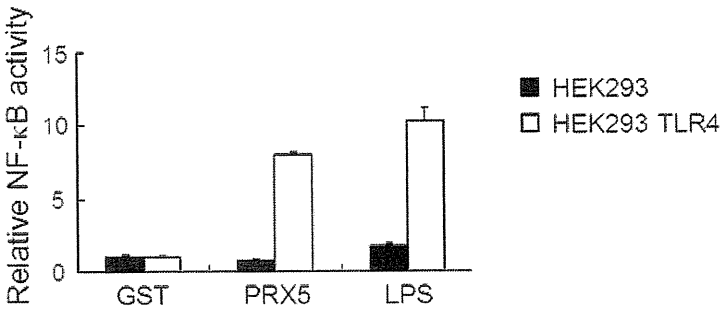

Supplementary Figure 9. The relative NF-κB activity in HEK293 or HEK293 TLR4 cell line by NF-κB luciferase assay 1 hour after stimulation by GST or PRX5 protein (1 μM) or LPS (100 ng ml^{-1}).

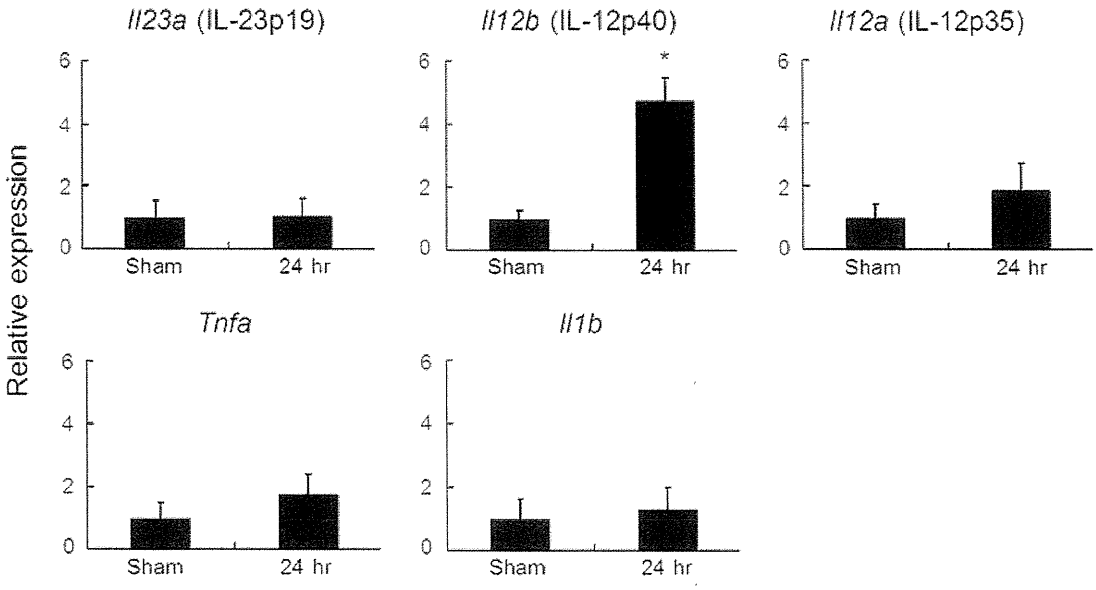

Supplementary Figure 10. The mRNA expression levels of inflammatory cytokines in peripheral blood monocytes of sham-operated mice or mice 24 hours after the induction of brain ischemia (n = 3 for each). *p < 0.05 vs. Sham [two-sided Student's t-test; error bars represent s.e.].

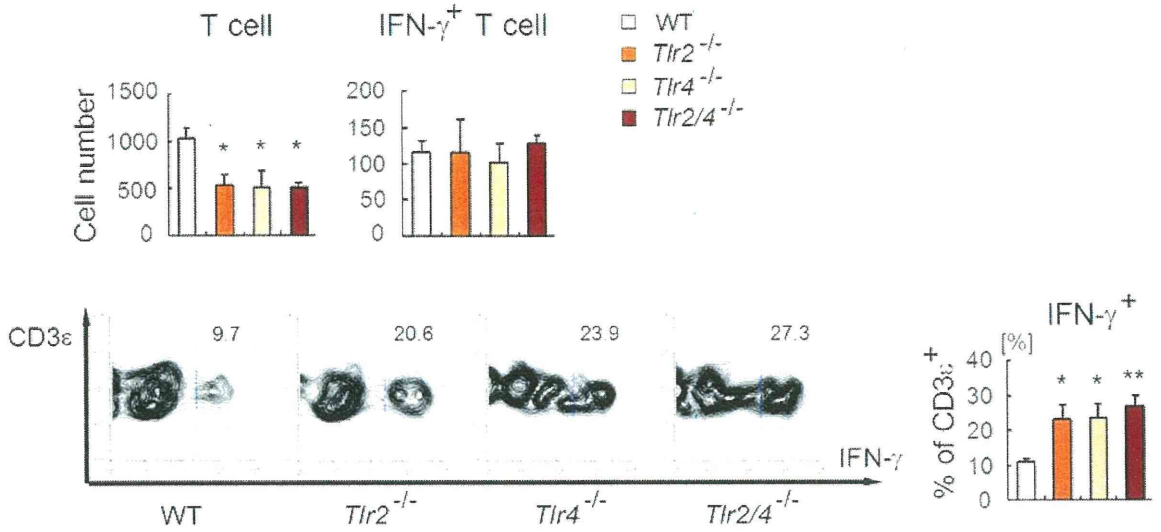

Supplementary Figure 11. The absolute number and the ratio of IFN-γ^+ T cell on day 3 (n = 8 for WT and n = 6 for other samples). TLR2 and/or TLR4 deficiency significantly increased the ratio of IFN-γ^+ T cells, because the number of IFN-γ^+ T cells was kept in spite of decreased number of total infiltrating T cells. *p < 0.05, **p < 0.01 vs WT (one-way ANOVA with Dunnett's correction; the error bars represent s.e.).

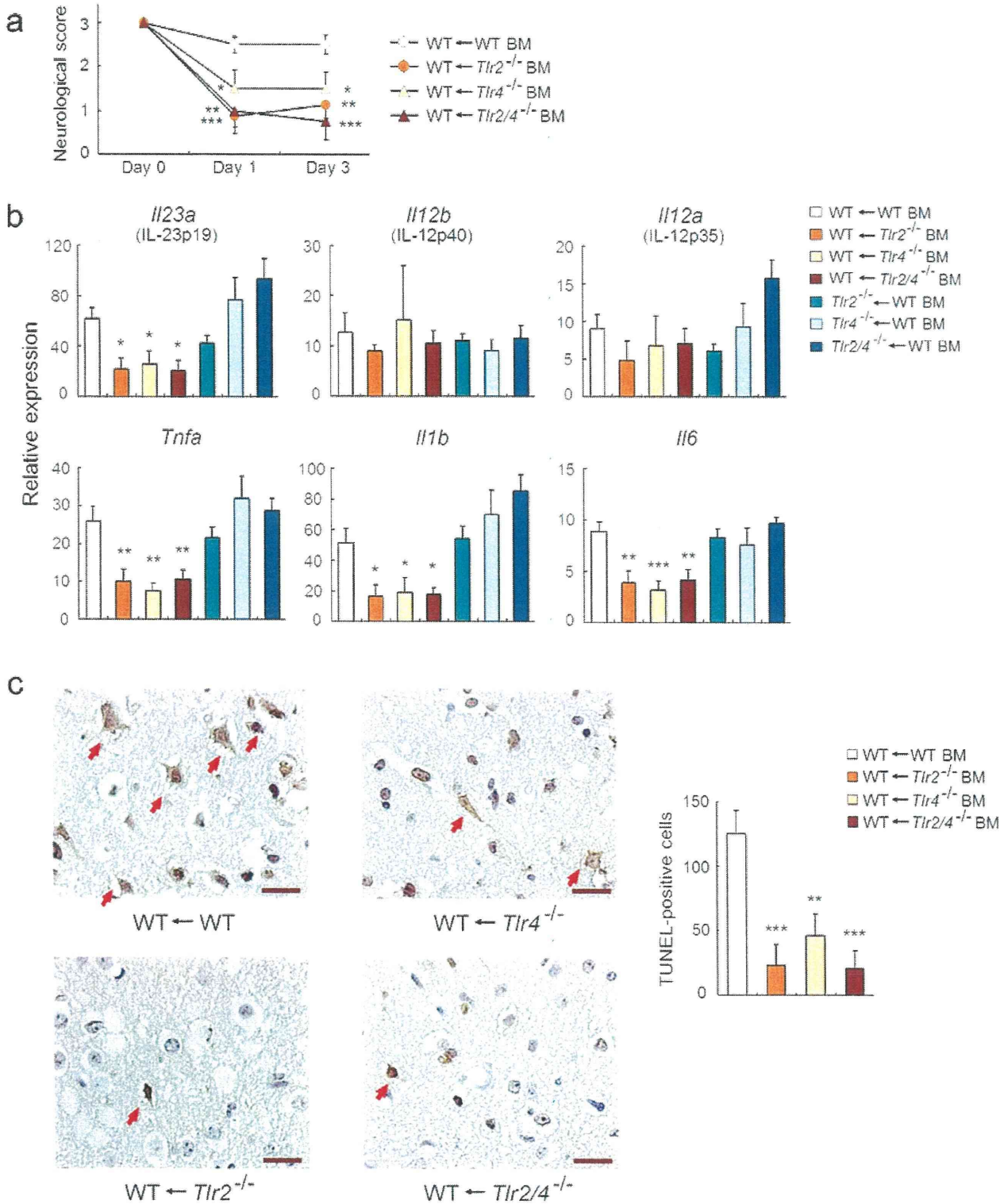

Supplementary Figure 12. (**a**) Neurological scores of WT or TLR-KO BM chimeric mice on days 1 and 3. (**b**) The mRNA expression levels of inflammatory cytokines in the infiltrating immune cells of WT or TLR-KO BM chimeric mice on day 1. (**c**) The results of TUNEL staining of the

peri-infarct area on day 4 (bar: 50 μm). The number of positive cells within three 0.1 mm^2 areas in the peri-ischemic parietal cortical region was expressed as an average value. $*p < 0.05$, $**p < 0.01$, $***p < 0.001$ vs. WT BM-transferred WT mice (one-way ANOVA with Dunnett's correction; the error bars represent s.e.).

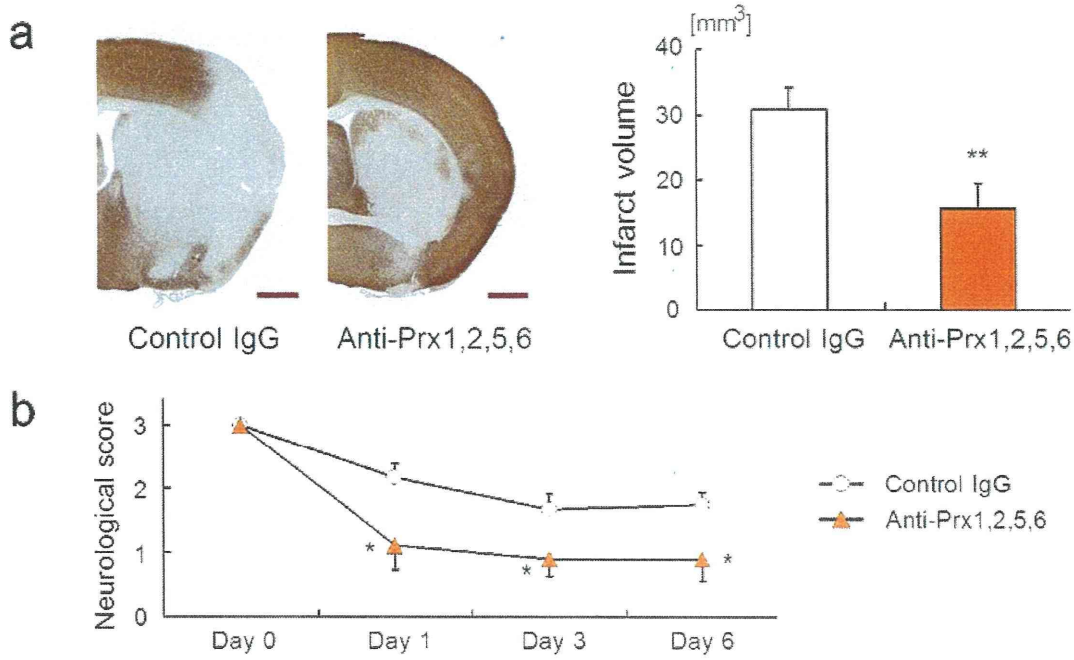

Supplementary Figure 13. (**a**) Infarct volume on day 7 (bar: 1 mm) and (**b**) neurological scores on days 1, 3, and 6 of mice treated with control IgG or anti-Prx antibody mixture just after the induction of brain ischemia (500 μg/mouse). *$p < 0.05$, **$p < 0.01$ vs. control IgG-administered mice (two-sided Student's *t*-test; the error bars represents s.e.).

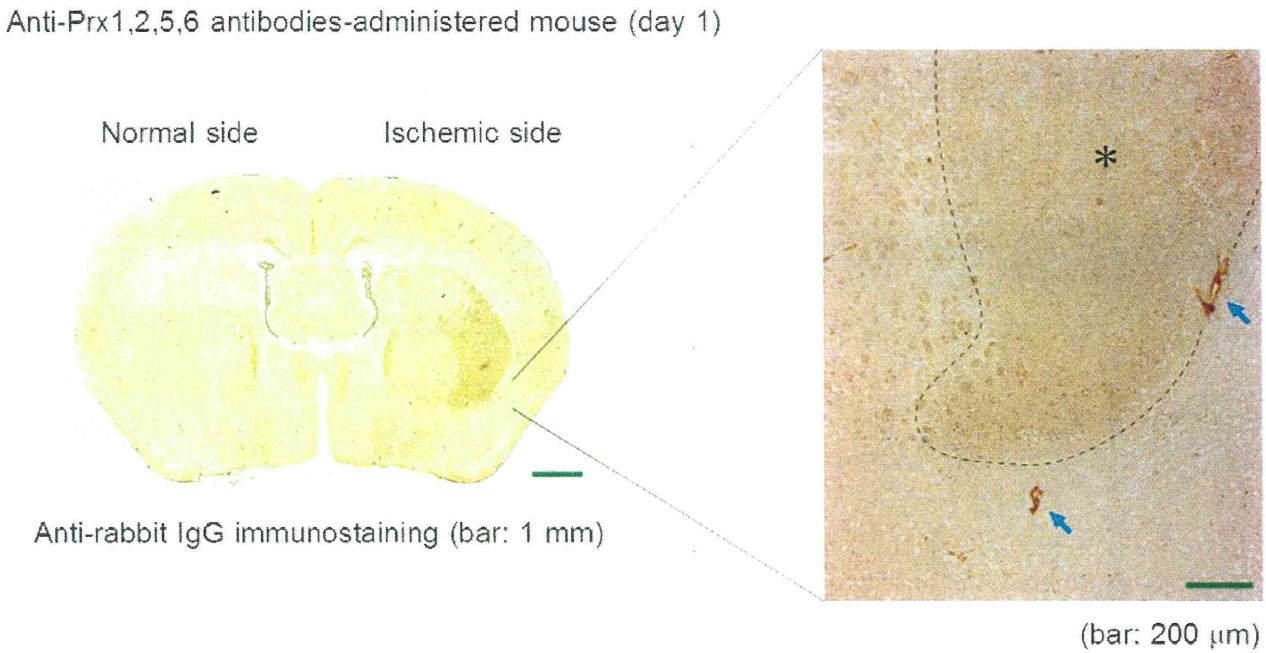

Supplementary Figure 14. The result of anti-rabbit IgG immunohistostaining of ischemic brain tissue on day 1. Positively stained region was observed in the ischemic area (*) and vascular lumen (blue arrow). Anti-Prx1,2,5,6 antibodies (derived from rabbit) were administered just after the induction of brain ischemia.

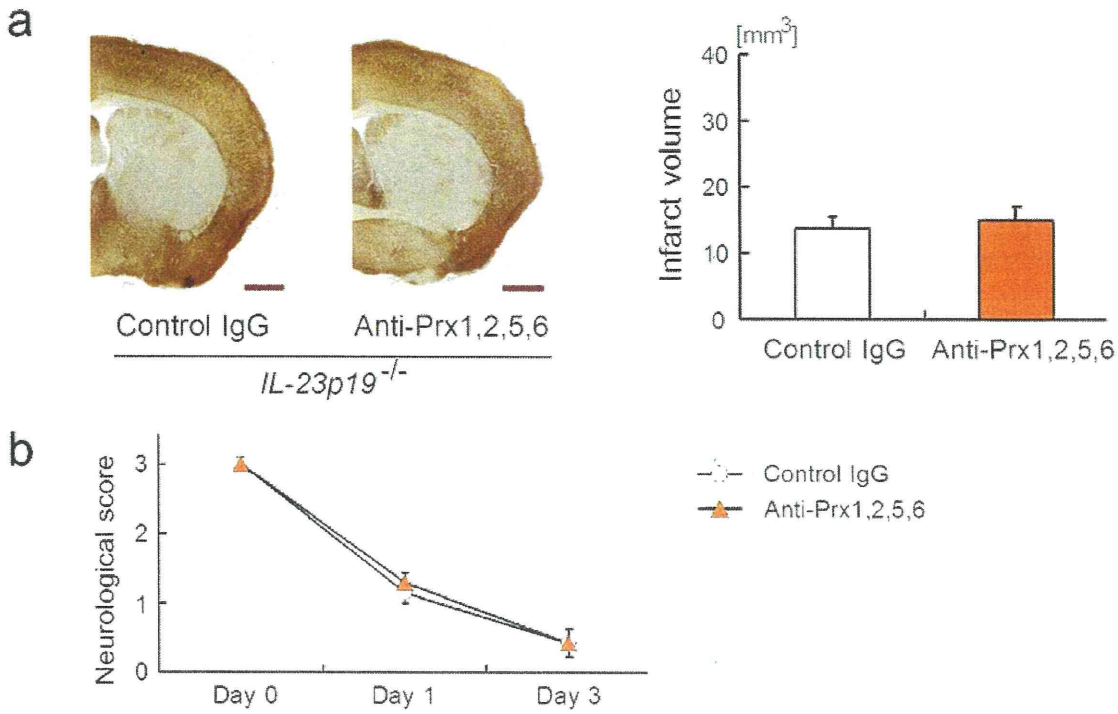

Supplementary Figure 15. (**a**) Infarct volume on day 4 (bar: 1 mm) and (**b**) neurological scores on days 1 and 3 of IL-23p19 KO mice treated with control IgG or anti-Prx antibody mixture just after the induction of brain ischemia (500 μg/mouse). There were no significant differences between control IgG- and anti-Prx antibody mixture-administered IL-23p19 KO mice (*n* = 7, each).

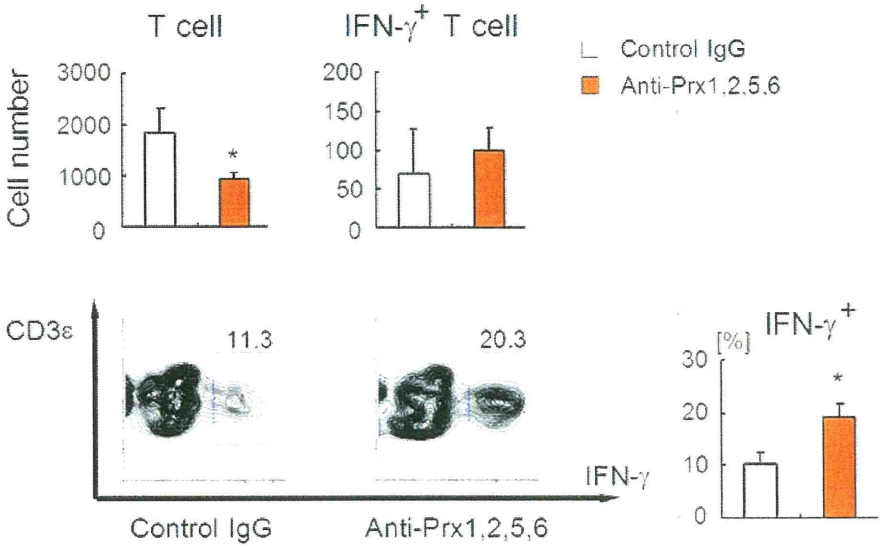

Supplementary Figure 16. The absolute number and the ratio of IFN-γ^+ T cell on day 3. The administration of anti-Prx antibody mixture significantly increased the ratio of IFN-γ-producing T cells, because the number of IFN-γ-producing T cells was kept in spite of decreased number of total infiltrating T cells, similar to TLR2 and/or TLR4 deficient mice (**Supplementary Fig.11**). *p < 0.05 vs. control IgG-administered mice (two-sided Student's t-test; the error bars represents s.e.).

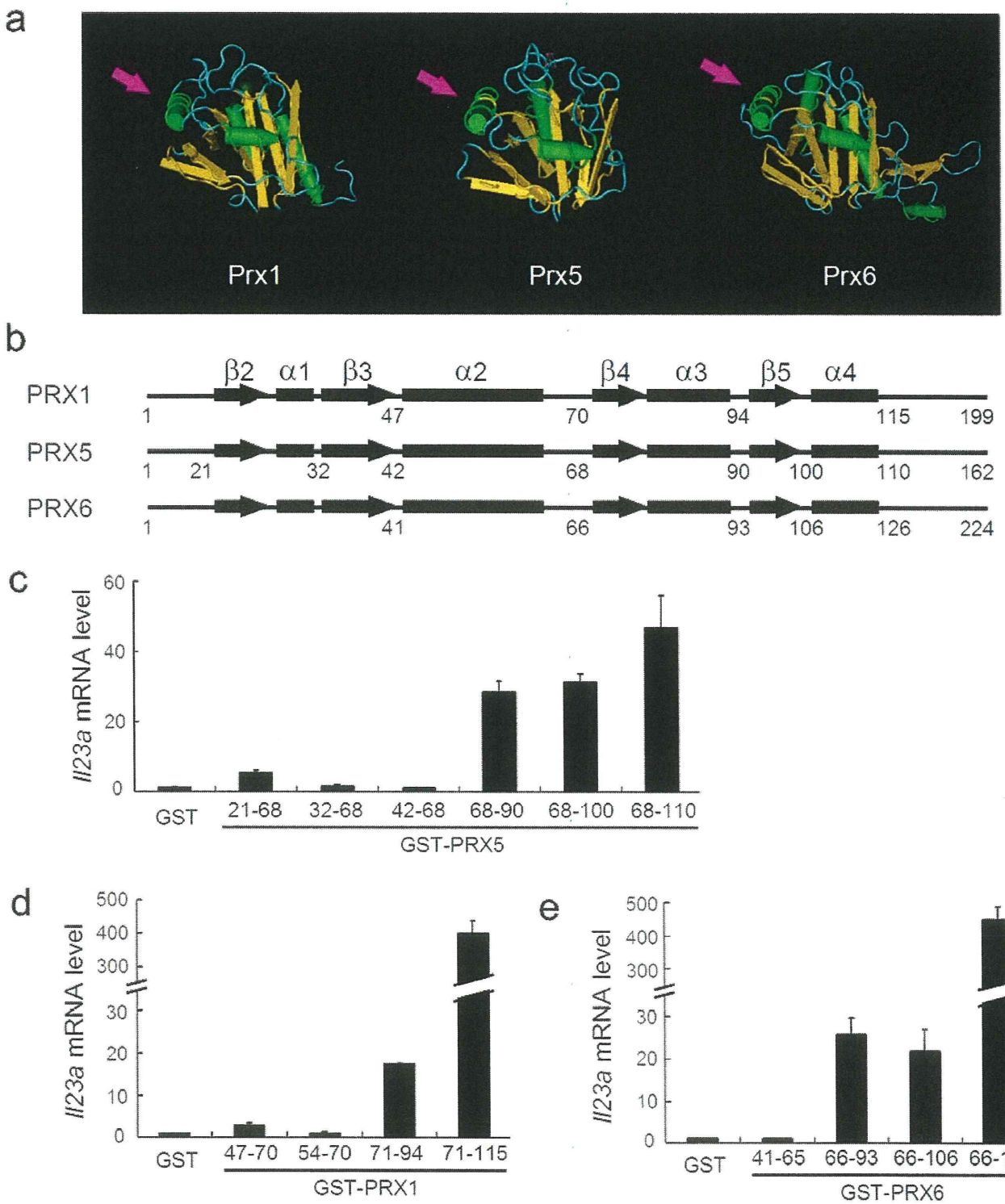

Supplementary Figure 17. (**a**) The crystal structure of Prx1 (Hbp23: rat homologue of Prx1; MMDB ID:11298), Prx5 (human Prx5; MMDB ID:26393), and Prx6 (hORF6: human homologue of Prx6; MMDB ID: 7978). Pink arrows indicate α3-helix of peroxiredoxins. They are relatively

sequestered on the protein surface and they are on almost opposite side of site for peroxidase activity. (**b**) The protein secondary structure of Prx family proteins. Numerals under the bar indicate amino acid residue numbers of each Prx protein. (**c,d,e**) IL-23p19-inducing activities of GST fusion PRX5 (**c**), PRX1 (**d**), and PRX6 (**e**) peptides. The number of amino acid residues contained in each PRX peptide was shown in X-axis. All of the IL-23p19 mRNA expression levels were detected by means of quantitative RT-PCR in BMDC 1 hour after the stimulation.

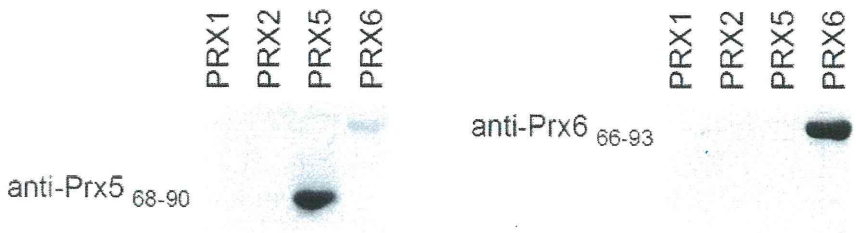

Supplementary Figure 18. Western blot analysis using rabbit polyclonal anti-Prx5 $_{68-90}$ and anti-Prx6 $_{66-93}$ antibody.

a

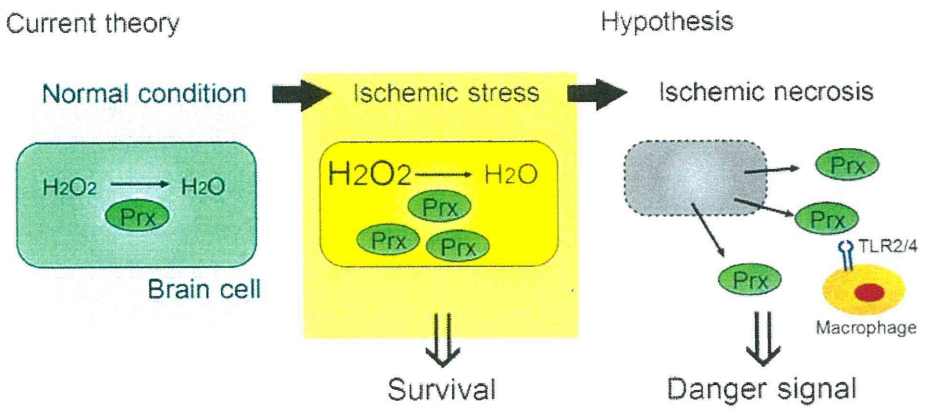

b

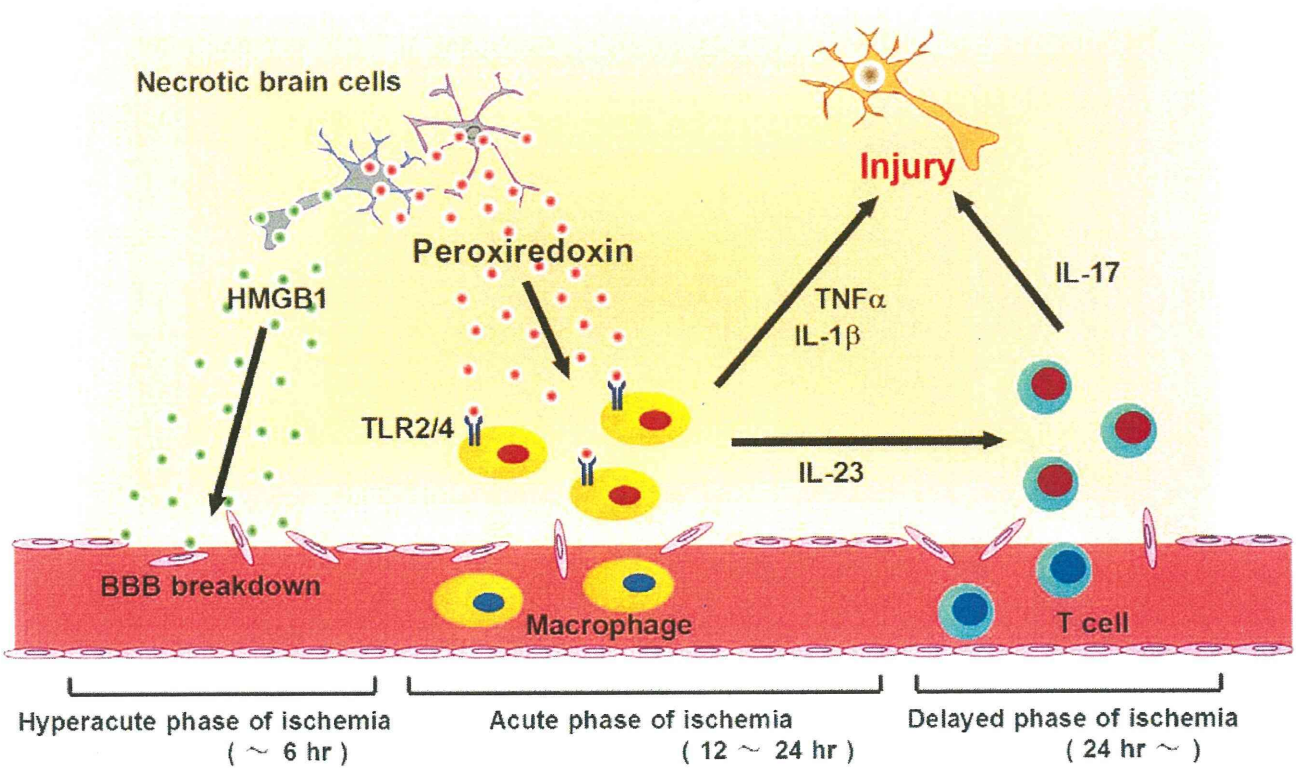

Supplementary Figure 19. Schematic model of the roles of DAMP molecules and inflammatory cytokines in the ischemic brain injury. (**a**) Peroxiredoxin (Prx) has two opposing functions: one inside and one outside the brain cells. Ischemic stress increases Prx expression inside brain cells, which may contribute to the survival of brain cells by catabolizing reactive oxygen species (ROS). But when ischemic phenomena finally results in the necrosis, Prx is released from necrotic brain cells into the extracellular compartment where it becomes a strong TLR2/4 stimulator for the infiltrating macrophages. (**b**) At the hyperacute phase of brain ischemia (within 6 hours after stroke onset), HMGB1 is released from ischemic brain cells and promotes

blood-brain barrier breakdown. Thereafter, peripheral blood cells begin to infiltrate into the ischemic brain, however, the extracellular release of HMGB1 is mostly diminished in the ischemic core at the acute phase of ischemia (12 to 24 hours after stroke onset). In this phase, extracellular Prx released from necrotic brain cells activates the infiltrating macrophages via TLR2/4 and induces the inflammatory cytokine expression which promotes ischemic injury. At the delayed phase of brain ischemia (over 24 hours after stroke onset), IL-23 induces IL-17 production from T cells ($\gamma\delta$T cells) and causes the further ischemic damages. Thus, HMGB1 is a hyperacute DAMP (within 6 hours after stroke onset), while Prx is the secondary one in the acute phase (12 to 24 hours after stroke onset) for postischemic inflammation.

Fraction	No. 2	No. 3
Phosphoglycerate kinase 1 (Pgk1)	11	10
Cofilin-1 (Cfl1)	10	4
Transgelin-3 (Tagln3)	9	5
Peptidyl-prolyl cis-trans isomerase (Ppia)	8	8
Triosephosphate isomerase (Tpi1)	7	10
Peroxiredoxin-5 (Prx5)	7	7
Fatty acid-binding protein, epidermal (Fabp5)	7	5
Carbonyl reductase [NADPH] 1 (Cbr1)	7	5
Alpha-synuclein (Snca)	6	5
Dual specificity protein phosphatase 3 (Dusp3)	6	3
Peroxiredoxin-6 (Prx6)	5	9
Gamma-synuclein (Sncg)	5	2
Alcohol dehydrogenase (Akr1)	5	6

Supplementary Table 1. The protein list identified by LC/MS analysis in No.2 and 3 sucrose gradient fraction.

	WT	TLR2 KO	TLR4 KO	TLR2/4 DKO
MABP (mmHg)	84 ±3	81 ±1	81 ±2	82 ±1
pH	7.33 ±0.01	7.35 ±0.02	7.33 ±0.02	7.33 ±0.01
PaO_2 (mmHg)	123 ±4	118 ±8	125 ±5	133 ±3
$PaCO_2$ (mmHg)	39.3 ±2.7	39.3 ±3.6	38.4 ±1.3	37.7 ±1.0
Hematocrit (%)	40.3 ±2.9	38.3 ±2.2	41.3 ±2.7	40.0 ±0.6

Supplementary Table 2. Physiological data of each type of mouse used in this study (average ± standard error, n = 3). MABP: Mean arterial blood pressure.

CBF reduction (%)	N	before CCA occlusion	after CCA occlusion	after MCA occlusion
WT	6	100	80.9 ± 3.7	14.3 ± 1.2
TLR2 KO	6	100	75.0 ± 4.0	16.5 ± 1.4
TLR4 KO	6	100	75.4 ± 3.1	14.9 ± 1.6
TLR2/4 DKO	6	100	74.2 ± 3.7	17.7 ± 2.2

Supplementary Table 3. The percent of cerebral blood flow (CBF) reduction after common carotid artery (CCA) occlusion and middle cerebral artery (MCA) occlusion (average ± standard error).

CBF reduction (%)	N	before CCA occlusion	after CCA occlusion	after MCA occlusion
WT ←WT BM	6	100	71.4 ± 5.0	13.5 ± 2.0
WT ←TLR2KO BM	6	100	76.2 ± 2.1	12.7 ± 2.6
WT ←TLR4KO BM	6	100	76.0 ± 3.2	14.7 ± 1.1
WT ←TLR2/4DKO BM	6	100	76.2 ± 3.0	13.3 ± 1.7
TLR2KO ←WT BM	6	100	80.4 ± 2.3	16.0 ± 1.0
TLR4KO ←WT BM	6	100	71.9 ± 3.0	15.1 ± 1.8
TLR2/4DKO ←WT BM	6	100	75.2 ± 3.2	13.7 ± 2.2

Supplementary Table 4. The percent of CBF reduction after CCA and MCA occlusion (average ± standard error).

a

CBF reduction (%)	N	before CCA occlusion	after CCA occlusion	after MCA occlusion
Control IgG	6	100	79.6 ± 4.0	16.2 ± 2.4
Anti-Prx1,2,5,6	6	100	75.2 ± 5.7	12.6 ± 0.8
Anti-HMGB1	6	100	78.2 ± 2.8	16.6 ± 1.9
Anti-HMGB1 + Prx	6	100	72.7 ± 2.1	12.9 ± 0.9

b

Survival rate (%)	N	Day 1	Day 4
Control IgG	17	100	94.1
Anti-Prx1,2,5,6	9	100	100
Anti-HMGB1	9	100	100
Anti-HMGB1 + Prx	9	100	100

Supplementary Table 5. (**a**) The percent of CBF reduction after CCA and MCA occlusion and (**b**) the survival rate of each type of mouse used in **Figure 4a,b** (average ± standard error).

Supplementary Methods

Bone marrow-chimeric mice. The recipient mice were given lethal doses of total body radiation with two 5 Gy exposures given four hours apart. The irradiated recipients were rescued by injecting the donor bone marrow cells (1×10^7) into the tail vein. Seven weeks after irradiation and bone marrow transplantation, bone marrow-chimeric mice were applied to the focal brain ischemia experiments.

Preparation of infiltrating immune cells. The mice were perfused with PBS transcardially. The forebrain was removed and well-suspended with RPMI-1640. The suspension was digested with type IV collagenase (1 mg ml^{-1}, Sigma-Aldrich) and DNase I (50 μg ml^{-1}, Roche) at 37°C for 45 minutes in a shaker. Infiltrating immune cells were isolated by 37%-70% Percoll (GE Healthcare) density gradient centrifugation and were removed from the interphase for further analysis.

FACS analysis. The method for surface and intracellular cytokine staining was described previously[2]. FACS analysis was performed on a FACSCantoII instrument (BD Biosciences) and analyzed using FlowJo software (Tree Star).

Generation of BMDC. Bone marrow was collected from tibias and femurs of C57BL/6 mice, TLR2- and/or TLR4-KO mice. Bone marrow cells were passed through a nylon mesh and cultured for eight days in RPMI-1640 medium with 10% fetal calf serum (FCS) and 1% supernatant from a granulocyte macrophage colony stimulating factor (GM-CSF) expressing cell line (J558L). The cytokine production was determined by quantitative real-time PCR or ELISA (eBioscience) at the indicated time points.

Quantitative real-time PCR. BMDCs or infiltrating inflammatory cells prepared by Percoll gradient centrifugation were lysed in RNAiso (Takara). Real-time PCR was performed on cDNA samples using KAPA SYBR Fast qPCR kit (Kapa Biosystems). The relative quantitation value is expressed as $2^{-\Delta Ct}$, where ΔCt is the difference between the mean Ct value of duplicate measurements of the sample and the endogenous hypoxanthine phosphoribosyltransferase 1 (HPRT1) control.